

$(A_m B_n)_x$ copolymers: A computational study of electronic and excitonic properties of quasi-one-dimensional superlattices

M. Seel

*Department of Physics, Michigan Technological University, Houghton, Michigan 49931
and Lehrstuhl für Theoretische Chemie, Friedrich-Alexander-Universität Erlangen-Nürnberg, Egerlandstrasse 3,
D-8520 Erlangen, West Germany*

C. M. Liegener, W. Förner, and J. Ladik

*Lehrstuhl für Theoretische Chemie, Friedrich-Alexander-Universität Erlangen-Nürnberg, Egerlandstrasse 3,
D-8520 Erlangen, West Germany*

(Received 20 May 1987)

Periodic copolymers representing quasi-one-dimensional superlattices $(A_m B_n)_x$ have been studied within the tight-binding approximation. The linear-combination-of-atomic-orbitals (LCAO) approach was used to calculate the splitting into subbands, the widths of the subbands, and the number of subbands in the well as a function of segment lengths m and n (barrier and well width). The Stark shift of subbands and the perturbed Wannier functions for a $(A_{16} B_{32})_x$ superlattice have been calculated for various electric field strengths using perturbation theory. Exciton resonances and the shift in exciton excitation energies due to an applied electric field have been computed by using a Pariser-Parr-Pople parameter for the electron-hole interaction. The parameters for the empirical tight-binding calculations were determined from fully self-consistent Hartree-Fock calculations and first-principles Green's function calculations for the exciton energies for superlattices of shorter segment lengths. For the Stark shift of the exciton peak a red shift of ~ 25 meV for 2×10^5 V/cm is calculated, similar to the shifts calculated and observed in three-dimensional superlattices.

I. INTRODUCTION

Semiconducting superlattices or quantum-well structures have been studied extensively in recent years.¹ These artificial structures are made by the alternating epitaxial growth of thin layers of two semiconductors and are currently of great technological interest with possible applications as semiconductor diode lasers,² electro-optical modulators,³ and nonlinear optical devices.⁴ In this paper we study the electronic structure of polymeric quasi-one-dimensional superlattices. They are not yet synthesized, but their realization as copolymers with a periodic sequence of m monomeric units A and n monomeric units B is conceivable, perhaps by using the Langmuir-Blodgett or the Merrifield synthetic technique.⁵ Copolymers having a *random* sequence of the constituent monomers A and B have already been synthesized, for example, copolymers of pyrrole with N -methyl-pyrrole⁶ or pyrrole with thiophene.⁷ A discussion of their electronic structure is given in Ref. 8.

Several theoretical approaches have been used to calculate the band structure of superlattices. Early experimental results could be explained qualitatively by means of simple quantum wells and Kronig-Penney models.⁹⁻¹¹ Other approaches are the envelope-function approximation,^{12,13} the tight-binding method,¹⁴⁻¹⁶ a Green's function theory,¹⁷ momentum Bloch functions,^{18,19} and \mathbf{k} - \mathbf{p} theory.²⁰⁻²² The effect of an electric field (perpendicular to the layers) on the subbands and exciton resonance energies has been studied using exact numerical solutions,²³

perturbation, and variational calculations²⁴⁻²⁶ in order to explain the large shifts and persistence of the exciton peaks due to the confinement of carriers. The dominant contribution to the observed red shift is the shift of the single-particle electron and hole energies. The decrease of the exciton binding energy due to the induced spatial separation between electrons and holes has less influence on the peak position.²⁵

Our objective is to investigate the new electronic properties of quasi-one-dimensional superlattices, possible modifications of the electronic and optical properties, and differences to three-dimensional quantum-well structures. This should provide us with guidelines for the molecular engineering of organic polymers with tailor-made properties. The linear-combination-of-atomic-orbitals (LCAO) tight-binding (Hückel) approach is used to study the electronic properties. For the study of the band structure of the constituent materials and for superlattices of shorter segment lengths the full *ab initio* self-consistent-field (SCF) Hartree-Fock (HF) solution²⁷ is obtained. The lowest exciton energy is calculated by using a first-principle charge transfer exciton formalism²⁸ which is based on Takeuti's intermediate exciton theory²⁹ and bridges the gap between the localized Frenkel exciton and the Wannier-Mott exciton with a large radius. This is important for organic polymers because, due to the strong covalent interaction between the monomeric unit cells, intracellular and intercellular excitations must be treated on the same footing. These first-principles SCF HF band-structure and exciton cal-

culations provide a check for the parameters used in the simple tight-binding calculations for superlattices with larger segment lengths. They show to what extent it is permissible to use the same parameters for the superlattice calculations as for the band-structure calculation of the constituent materials. They also provide a “reasonable” coupling parameter for the interface region.

The paper is organized as follows. In Sec. II method and computational details are described. Section III gives the results. In Sec. III A the HF band-structure and exciton calculations are discussed. The results for the superlattices with $(A_{16}B_{32})$ as the largest unit cell, and for the perturbation calculation of the quadratic Stark shift of the exciton peaks, are presented in Sec. III B. Finally, in Sec. IV a summary and the conclusions are given.

II. METHOD AND COMPUTATIONAL DETAILS

A. Summary of Hartree-Fock and exciton theory expressions

To assess the applicability of the one-orbital-per-site non-self-consistent tight-binding method for superstructures of larger segment lengths, the SCF HF LCAO method for infinite periodic polymers²⁷ is employed to calculate the band structure of the constituent materials and of the quantum-well structures of shorter segment lengths. In this method a Bloch wave function $\psi_n(\mathbf{k}, \mathbf{r})$ is represented as

$$\psi_n(\mathbf{k}, \mathbf{r}) = \sum_i c_{in}(\mathbf{k}) \phi_i(\mathbf{k}, \mathbf{r}) \quad (1)$$

with

$$\phi_i(\mathbf{k}, \mathbf{r}) = \frac{1}{\sqrt{N}} \sum_{\mu} e^{i\mathbf{k} \cdot \mathbf{R}_{\mu}} u_i(\mathbf{r} - \mathbf{R}_{\mu}), \quad (2)$$

$u_i(\mathbf{r} - \mathbf{R}_{\mu}) = u_i^{\mu}$ being the i th atomic orbital centered in cell μ .

The advantage of the LCAO description is that the coefficients in the wave function (either as Bloch or Wannier function) yield immediately a picture of its physical properties: for example, for a miniband near the bottom of the well, nonzero coefficients for atomic orbitals centered on sites in the low-gap material and vanishing amplitudes in the high-gap material describe a wave function which allows for resonant tunneling^{5,30,31} of an electron through the array of these wells and barriers.

The energy bands and wave functions are determined from the self-consistent solution of the HF equation

$$\underline{F}(\mathbf{k})c_n(\mathbf{k}) = E_n(\mathbf{k})\underline{S}(\mathbf{k})c_n(\mathbf{k}). \quad (3)$$

The Fock matrix elements

$$F_{ij}(\mathbf{k}) = \sum_{\mu} e^{i\mathbf{k} \cdot \mathbf{R}_{\mu}} F_{ij}^{0\mu}, \quad (4)$$

with

$$F_{ij}^{0\mu} = h_{ij}^{0\mu} + g_{ij}^{0\mu}, \quad (5)$$

are constructed from the one-electron matrix elements $h_{ij}^{0\mu}$,

$$h_{ij}^{0\mu} = -\frac{1}{2} \langle u_i^0 | \Delta | u_j^{\mu} \rangle - \sum_{\nu} \sum_A \left\langle u_i^0 \left| \frac{Z_A}{|\mathbf{r} - \mathbf{R}_{\nu} - \mathbf{R}_A|} \right| u_j^{\mu} \right\rangle, \quad (6)$$

and two-electron matrix elements $g_{ij}^{0\mu}$,

$$g_{ij}^{0\mu} = \sum_{\lambda} \sum_{\nu} \sum_l \sum_m P_{lm}^{\lambda\nu} \left[2 \begin{bmatrix} 0\mu & \lambda\nu \\ ij & lm \end{bmatrix} - \begin{bmatrix} 0\lambda & \mu\nu \\ il & jm \end{bmatrix} \right]. \quad (7)$$

The computation of the exciton band $E(\mathbf{K})$ consists of the following steps.²⁸

(i) Transformation of the Bloch functions to Wannier functions

$$W_n(\mathbf{r} - \mathbf{R}_{\mu}) = \frac{1}{\sqrt{N}} \sum_{\mathbf{k}} e^{-i\mathbf{k} \cdot \mathbf{R}_{\mu}} \psi_n(\mathbf{k}), \quad (8)$$

and calculation of the matrix \underline{V} of the electron-hole (e - h) interaction. This involves basically two-electron integrals of the type given in Eq. (7), but integrals over Wannier functions instead of atomic orbitals. The lower-lying triplet exciton state is determined by Coulomb-type integrals $-J_{vc}$ (v and c stand for valence and conduction band, respectively). For the singlet state, additional exchange terms $2K_{vc}$ shift the singlet state to higher energies.^{29,32}

(ii) Calculation of the Green matrix $\underline{G}(E)$:

$$G[\mathbf{R}_{\mu}, \mathbf{R}_{\nu}, E(\mathbf{K})] = \frac{1}{N} \sum_{\mathbf{k}} \frac{\exp[i\mathbf{k} \cdot (\mathbf{R}_{\mu} - \mathbf{R}_{\nu})]}{E(\mathbf{K}) - [E_c(\mathbf{k}) - E_v(\mathbf{k} - \mathbf{K})]}. \quad (9)$$

(iii) The zeros of the determinant $D = |\underline{1} - \underline{G}\underline{V}|$ determine the exciton energy $E(\mathbf{K})$.

B. Computational details for *ab initio* calculations

The simplest quasi-one-dimensional systems which allow, on the *ab initio* level, for the modeling of low- and high-energy gap polymers, for superlattices with any reasonable unit-cell size, and for exciton calculations of the type described above are chains of Li and H atoms. These model systems served as test cases for HF calculations of infinite periodic systems.³³ For the present study the simplest possible approximations are used. To model a low-gap polymer a linear Li chain with alternating bond distances d_1 , d_2 , and $d_1 + d_2 = 6.06$ Å (twice the nearest-neighbor separation in a bcc Li metal) is used. The degree of bond alternation determines the value of the fundamental gap. A linear hydrogen chain with alternating bond distances ($d_1 + d_2 = 1.95$ Å) serves as a model for a high-gap semiconducting polymer. The basis set is an STO-3G basis (two functions on Li, one s function on H, each constructed from three Gaussians³⁴). Using this minimal basis, Hartree-Fock and exciton calculations for a $(\text{Li}_{12}\text{H}_4)_x$ quantum-well structure (28 orbitals per unit cell, well width of ~ 36 Å, barrier

width of $\sim 4 \text{ \AA}$, "interface" Li-H distance of $\sim 3 \text{ \AA}$ are quite feasible.

C. Tight-binding (Hückel) expressions

The energy bands of the π electrons of conjugated polyene chains represent, within the framework of the Hückel approximation, the simplest case of a spectrum which consists of a valence and conduction band. If the alternating bonds are described by resonance or hopping parameters β_1 and β_2 , the allowed energy bands are³⁵

$$\begin{aligned} E_v(k) &= \alpha - (\beta_1^2 + \beta_2^2 + 2\beta_1\beta_2 \cos k)^{1/2}, \\ E_c(k) &= \alpha + (\beta_1^2 + \beta_2^2 + 2\beta_1\beta_2 \cos k)^{1/2}. \end{aligned} \quad (10)$$

Both bands have a width of $2|\beta_2|$ and are separated by a gap $\Delta E = 2|\beta_1 - \beta_2|$. The "on-site" parameter α fixes the position of the band (see Fig. 1). Therefore, by a suitable choice of the parameters α , β_1 , and β_2 , a variety of two-band systems (constituent materials of the superlattice) which differ in bandwidths, band gaps, and relative positions of the band gaps can be modeled.

Once the parameters are fixed ("tuned" to the *ab initio* or experimental¹⁴ valence- and conduction-band structure), the same parameters are used for the calculation of the band structure of a superlattice. The only variable

parameter is the hopping parameter which describes the coupling between segments *A* and *B*.

After diagonalizing the tight-binding or Hückel matrix for a $(A_m B_n)_x$ superlattice with $m+n=l$ sites in the unit cell, the Bloch function is

$$\psi_j(k, \mathbf{r}) = \frac{1}{\sqrt{N}} \sum_{i=1}^l c_{ij}(k) \sum_{\mu} e^{ikR_{\mu}} u_i(\mathbf{r} - \mathbf{R}_{\mu}). \quad (11)$$

μ denotes a unit cell of the superlattice, *i* an individual site in the unit cell (one orbital per site). The specific form of u_i^{μ} is unimportant. For the evaluation of matrix elements in the perturbation calculations described below, only certain symmetry restrictions with respect to the form of the orbital apply. To compute Wannier functions, the undetermined phase of the Bloch function can be chosen so as to obtain real, highly localized Wannier functions (see Ref. 28 and references therein). In the case of the superlattices considered here, the LCAO coefficients $c_{ij}(k)$ of low-lying minibands show almost no dispersion, $c_{ij}(k=0) \sim c_{ij}(k=\pi/a)$. Wannier functions which approximate the exact function quite accurately can be constructed in a very simple way, starting from Eq. (8) and using the summation relation for \mathbf{k} vectors in the Brillouin zone:

$$\begin{aligned} W_j(\mathbf{r} - \mathbf{R}_{\mu}) &\simeq \frac{1}{\sqrt{N}} \sum_{\mathbf{k}} e^{-ik \cdot \mathbf{R}_{\mu}} \frac{1}{\sqrt{N}} \sum_{\mathbf{v}} c_{ij}(k=0) \sum_{\mathbf{v}} e^{ik \cdot \mathbf{R}_{\mathbf{v}}} u_i(\mathbf{r} - \mathbf{R}_{\mathbf{v}}) \\ &= \frac{1}{N} \sum_{\mathbf{i}} c_{ij}(k=0) \sum_{\mathbf{v}} \sum_{\mathbf{k}} e^{-ik(\mathbf{R}_{\mu} - \mathbf{R}_{\mathbf{v}})} u_i(\mathbf{r} - \mathbf{R}_{\mathbf{v}}) \\ &= \frac{1}{N} \sum_{\mathbf{i}} c_{ij}(k=0) \sum_{\mathbf{v}} N \delta_{\mu\mathbf{v}} u_i(\mathbf{r} - \mathbf{R}_{\mathbf{v}}) \\ &= \sum_{\mathbf{i}} c_{ij}(k=0) u_i(\mathbf{r} - \mathbf{R}_{\mu}). \end{aligned} \quad (12)$$

Equation (12) shows that the Wannier function for a superlattice band *j* with almost no dispersion is localized within one unit cell. In addition, the LCAO coefficients give a direct measure of how far the tails of the Wannier function are extending from the well into the barrier.

Using the Wannier functions, the effect of an electric field perpendicular to the segments defining the quantum wells (along the polymer axis) can be calculated. The subbands E_n in the energy region of the conduction- (valence-) band discontinuity are the allowed energy states of a particle in a quantum well with a finite height, separated from another well by a barrier with a finite thickness. Perturbation theory to calculate the Stark shift is applicable if the shift in the energy subbands is small compared to the separation between two bands without a field. If the origin of the electrostatic potential is chosen at the center of a well, the second-order Stark shift due to a field in the *z* direction is given by

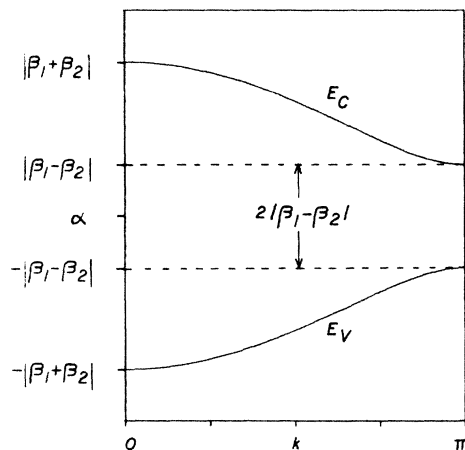


FIG. 1. The energy-band structure of an alternating-bond system described by hopping parameters β_1 and β_2 [see Eq. (10)].

$$\tilde{E}_n = E_n + (eE)^2 \sum'_m \frac{|\langle W_n | z | W_m \rangle|^2}{E_n - E_m}. \quad (13)$$

The perturbed Wannier function is then

$$\tilde{W}_n(\mathbf{r} - \mathbf{R}_\mu) = W_n + eE \sum'_m \frac{\langle W_n | z | W_m \rangle}{E_n - E_m} W_m(\mathbf{r} - \mathbf{R}_m). \quad (14)$$

Using Eq. (12) the matrix elements $\langle W_n | z | W_m \rangle$ become

$$\begin{aligned} \langle W_n | z | W_m \rangle &= \sum_{i,j} c_{in}(k=0)c_{jm}(k=0) \\ &\quad \times \langle u_i(\mathbf{r} - \mathbf{R}_\mu) | z | u_j(\mathbf{r} - \mathbf{R}_\mu) \rangle \\ &\equiv \sum_{i,j} c_{in}c_{jm} \langle u_i | z | u_j \rangle. \end{aligned} \quad (15)$$

If the atomic orbitals u_i are symmetric with respect to an axis which is perpendicular to the plane of the unit cell and goes through atom i and if overlap integrals are neglected, the matrix element is simply³⁶

$$\langle W_n | z | W_m \rangle = \sum_i c_{in}c_{im}z_i, \quad (16)$$

where z_i is the z coordinate of atom i .

To analyze the problem of the exciton energy we can treat the Coulomb interaction between the excited electron and the hole left behind in a first approximation as a perturbation, using as the zeroth-order wave function a product of the Wannier functions of the electron and the hole:

$$\begin{aligned} \hat{H}_0 &= \hat{H}_e + \hat{H}_h, \quad \psi^0 = |W_e W_h\rangle, \\ \hat{H}_{eh} &= -\frac{e^2}{r}. \end{aligned} \quad (17)$$

In first-order perturbation theory, the energy shift which defines the exciton binding energy E_{EXB} is given by

$$\begin{aligned} E_{\text{EXB}} &= \langle \psi^0 | \hat{H}_{eh} | \psi^0 \rangle = - \left\langle W_e W_h \left| \frac{e^2}{r} \right| W_e W_h \right\rangle \\ &= - \sum_{i,j,k,l} c_{ie}c_{jh}c_{ke}c_{lh} \left\langle u_i u_j \left| \frac{e^2}{r} \right| u_k u_l \right\rangle. \end{aligned} \quad (18)$$

The matrix elements can be evaluated as in the Pariser-Parr-Pole (PPP) approximation³⁷ (equivalent to a Hubbard Hamiltonian with on- and off-site Coulomb interaction):

$$E_{\text{EXB}} = - \sum_{i,j} c_{ie}^2 c_{jh}^2 \gamma_{ij}. \quad (19)$$

In the parametrization of Nishimoto and Mataga³⁸ γ_{ij} is given by

$$\gamma_{ij} = (d_{ij} + a_{ij})^{-1}, \quad a_{ij}^{-1} = \frac{1}{2}(\gamma_{ii} + \gamma_{jj}). \quad (20)$$

d_{ij} denotes the distance between atoms i and j . The Coulomb integral γ_{ii} for electrons on the same atom i is treated as a parameter, usually as the difference between

ionization potential and electron affinity value. In our case γ_{ii} is a parameter used to reproduce approximately the first exciton resonance as calculated from first principles, as described in Sec. II A. The resultant energy of the lowest exciton resonance is then

$$E_{\text{ex}} = E_e + E_h + E_{\text{EXB}}, \quad (21)$$

and the excitation energy for the first exciton absorption

$$E_{\text{abs}} = E_e + E_h + E_{\text{EXB}} - 2E_h = E_e - E_h + E_{\text{EXB}}. \quad (22)$$

The same expressions would have been obtained if one uses Takeuti's exciton formalism together with the fact that the valence- and conduction-band Wannier functions of a quantum-well structure are localized within one unit cell of the superlattice and excitations between wells across the barrier are highly improbable. The matrix and determinantal equations reduce to simple scalar relations:

$$\begin{aligned} 1 - GV &= 0, \\ 1 - [E - (E_e - E_h)]^{-1} E_{\text{EXB}} &= 0, \\ E &= E_e - E_h + E_{\text{EXB}}. \end{aligned} \quad (23)$$

Shifts in the exciton absorption energies due to an electric field can be calculated by substituting the perturbed energies and Wannier functions from Eqs. (13) and (14) in the above expressions. However, if we first apply perturbation theory to calculate the effect of the electric field on the electron and hole states (small effect), and then use this wave function in a second application of perturbation theory to take into account the electron-hole interaction (large effect if zero-field exciton binding energy is large), the results become unphysical for large zero-field exciton binding energies. A more consistent way to calculate approximately the Stark shift of the exciton peak is *not* to separate the problem of electron-hole interaction and electric field but to treat both effects simultaneously in the same order of perturbation theory:

$$\begin{aligned} \hat{H}_0 &= \hat{H}_e + \hat{H}_h, \\ \hat{H}_p &= eEz_e - eEz_h - e^2/r, \end{aligned} \quad (24)$$

using as unperturbed energies and states the energies and wave functions of the lowest electron-hole pairs:

$$\begin{aligned} E_0 &= E_e^1 + E_h^1, \quad \psi_0 = |W_e^1 W_h^1\rangle, \\ E_1 &= E_e^2 + E_h^1, \quad \psi_1 = |W_e^2 W_h^1\rangle, \\ E_2 &= E_e^1 + E_h^2, \quad \psi_2 = |W_e^1 W_h^2\rangle. \end{aligned} \quad (25)$$

The superscripts denote the n th electron and hole states in the quantum well. Our numerical calculations show that the Wannier functions have the same symmetry properties as the particle-in-a-box functions. Therefore quite a few matrix elements vanish. In first order, the exciton binding energy is obtained:

$$E^{(1)} = - \left\langle W_e^1 W_h^2 \left| \frac{e^2}{r} \right| W_e^1 W_h^1 \right\rangle = E_{\text{EXB}}, \quad (26)$$

in second order the quadratic Stark shift

$$E^{(2)} = -2(eE)^2 \frac{|\langle W_e^2 | z | W_e^1 \rangle|^2}{E_e^2 - E_e^1}, \quad (27)$$

but no field-dependent correction to the binding energy which is a higher-order correction is obtained. Therefore the excitation energy for the first exciton in the presence of an electric field is in second order,

$$E_{\text{abs}} = E_e - E_h + E^{(1)} + E^{(2)}. \quad (28)$$

This result is consistent with variational calculations of the quantum-confined Stark effect in three-dimensional quantum-well structures²⁵ which have shown that the dominant contribution, at least at higher fields, is the shift of the single-particle energies. This completes the LCAO tight-binding description of a quasi-one-dimensional superlattice and the Stark shift of the exciton absorption peak. Note that the only adjustable parameters are the hopping parameters β and the Coulomb integral γ . The number and the dispersion of the subbands in the well, the extent of the Wannier functions into the barrier segment, and the Stark shift of the valence and conduction band and of the exciton binding energy are determined by the lengths of the segments that define the well and the barrier structure.

III. RESULTS AND DISCUSSION

A. Hartree-Fock band structures and exciton energies

The results of the Hartree-Fock and exciton calculations are summarized in Fig. 2. The high-gap polymer is

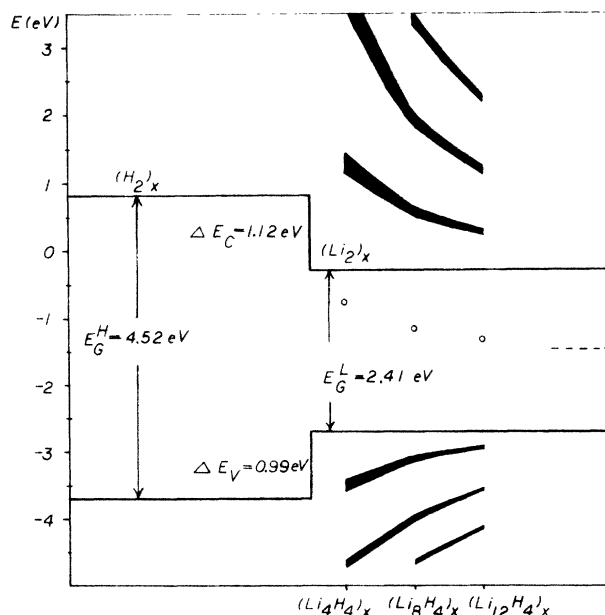


FIG. 2. The Hartree-Fock energy-band structure of $(H_2)_x$, $(Li_2)_x$, and two "superlattice" energy bands in the valence- and conduction-band region of the low-gap material as a function of well width ($Li_4 \cong \sim 12 \text{ \AA}$, $Li_8 \cong \sim 24 \text{ \AA}$, $Li_{12} \cong \sim 36 \text{ \AA}$) for a constant barrier width ($H_4 \cong \sim 6 \text{ \AA}$). The dashed range indicates the lower and upper limit of the minibands. The circles indicate the position of the lowest exciton level for the superlattices, the dashed line for the constituent material $(Li)_x$.

modeled by a chain of hydrogen atoms. A band gap of $\sim 4.5 \text{ eV}$ is obtained for $d_1 = 0.978 \text{ \AA}$, $d_2 = 0.974 \text{ \AA}$. The reason the gap is still quite large even for this small bond alternation is that even in the equidistant case a gap opens up, due to a charge-density wave. The width of the valence (conduction) band is $\sim 16 \text{ eV}$ (36 eV). For the Li chain the choice of $d_1 = 3.033 \text{ \AA}$, $d_2 = 3.027 \text{ \AA}$ yields a gap of $\sim 2.4 \text{ eV}$ and a valence- (conduction-) bandwidth of $\sim 2.6 \text{ eV}$ (5.8 eV). The conduction- and valence-band discontinuities which define the barrier height are 1.12 and 0.99 eV, respectively. Taking interactions up to five nearest neighbors of the (Li_2) unit cell into account, one obtains an exciton excitation energy of $\sim 1.25 \text{ eV}$ (binding energy of $\sim 1.15 \text{ eV}$). The band structure does not change essentially if at least three neighbor interactions are taken into account. The exciton energy, on the other hand, is still not fully converged. Extrapolation indicates an energy of $\sim 1.20 \text{ eV}$ for seven nearest-neighbors interactions. For the present investigation it is sufficient to know that the lowest exciton state lies approximately halfway in the gap. The values for the gaps of the constituent materials, the band discontinuities, and the exciton energy are representative values for actual polymer systems. The largest difference to three-dimensional systems is in the exciton binding energies: $\sim 4.2 \text{ meV}$ for GaAs, 8.6 meV for a heavy-hole exciton in the superlattice,²⁵ ~ 0.4 and $\sim 1.2 \text{ eV}$ for singlet and triplet excitons in polydiacetylenes.²⁸

Figure 2 also shows the SCF HF band structures of $(H_4Li_n)_x$ superlattices for $n = 4, 8$, and 12. The energy bands of the low-gap material are shown as a function of the number of Li atoms, i.e., for the well width (Li_4, Li_8 , and Li_{12} corresponding to $\sim 12, 24$, and 36 \AA , respectively) with a constant barrier consisting of four hydrogen atoms ($\sim 6 \text{ \AA}$ barrier width). The valence and the conduction bands of $(Li_2)_x$ break up into minibands or subbands with decreasing bandwidths for increasing n , e.g., 130, 70, and 50 meV for the top valence miniband for $n = 4, 8$, and 12. The separation between the top two valence bands decreases from ~ 1 to 0.5 eV, i.e., it is about ten times larger than the widths of these bands. For increasing n , the bands move slowly into the well region defined by the band-gap discontinuities. It is only for $n \geq 8$ that one valence and one conduction band fall into the well region.

The lowest-lying exciton resonances for these superlattices are indicated by circles in Fig. 2. Again they are about midway in the gap defined by the minibands. The excitation energy decreases from 2.66 to 1.89 to 1.63 eV for $n = 4, 8$, and 12, slowly approaching the value of 1.25 eV obtained for $(Li_2)_x$.

A Mulliken population analysis for the charge distribution shows that a slight charge redistribution occurs at the interface. The charges on the first four Li atoms are 2.96, 3.04, 2.99, and 3.01. Then the "bulk" value of 3.00 is reached. The values on the H atoms which represent the barrier are 1.01, 0.99, and, by symmetry, again 0.99 and 1.01. In agreement with investigations on three-dimensional systems,^{14,39-41} these corrections to the charge distribution are small enough to make it not unreasonable to proceed to tight-binding calculations

of larger superlattice structures using input parameters which are fitted to the band structures of the constituent materials.

B. Tight-binding results

In the tight-binding calculations, polymers with gaps and band discontinuities which are slightly lower than the *ab initio* values were modeled. Qualitatively, all the characteristic features of the first-principle SCF calculations are preserved. The parameters which describe the barrier material A are $\alpha^A=0$, $\beta_1^A=-10.155$, and $\beta_2^A=-8.085$. The corresponding parameters for the low-gap material B are $\alpha^B=-0.03$, $\beta_1^B=-2.475$, and $\beta_2^B=-1.325$. The resulting band discontinuities are indicated in Fig. 3. As the first trial value for β_{AB} , the parameter which describes the interaction between neighboring atoms A and B at the interface of the superlattice, -1 was chosen. This describes an interaction which is slightly weaker than the weak bond in the $(\text{Li}_2)_x$ system. The resulting superlattice energy bands are shown as a function of the well width and constant barrier in Fig. 3(a). For all practical purposes of the present investigation the qualitative agreement with the Hartree-Fock calculations for $n=4, 8$, and 12 is satisfactory and, therefore, no further optimization of β_{AB} was performed. The main difference from the HF calculations is that, as a consequence of Eq. (10), the minibands in the valence- and conduction-band regions are symmetric with respect to $\alpha=-0.03$ and have the same dispersion.

Going from $n=4$ to $n=32$ the dispersion decreases from 150 to 3 meV for the lowest-lying band (ground state of the well). Its position shifts from ~ 650 meV above the bottom of the well to about 40 meV. For $n=32$ the dispersions of the five minibands in the well are 3, 9, 16, 21, and 24 meV, respectively. The separations between the minibands are 112, 164, 196, and 213

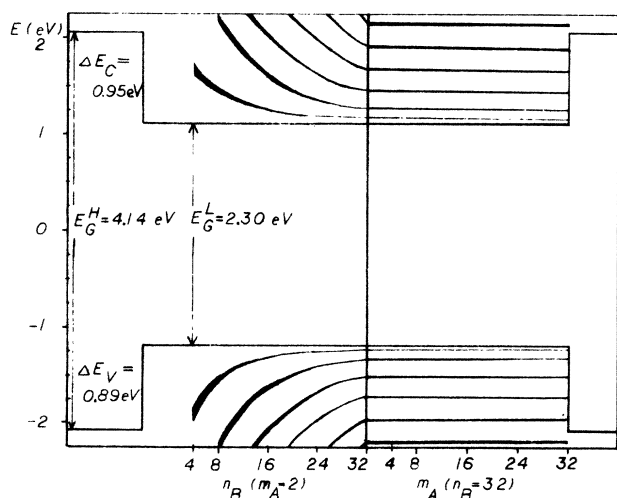


FIG. 3. The tight-binding band structures of $(A_m B_n)_x$ superlattices (a) as a function of well width for a constant barrier width A_2 and (b) as a function of barrier width for constant well width (B_{32}) .

meV. One consequence of the strong dependence of the band structure on the well width is that electron transport by miniband conduction will be strongly affected. The larger the low-gap polymer segment becomes, the smaller the bandwidth and, therefore, the larger the effective mass of the carriers will be, resulting in a decrease of conductivity. It was shown recently⁴² for a GaAs/AlAs double-barrier diode structure that the resonant tunneling current decreases by 2 orders of magnitude if the well width is increased from 5 to 9 nm.

On the energy scale of Fig. 3, the miniband structure as a function of the barrier width [see Fig. 3(b)] seems almost independent of the width of the barrier (number of A atoms). There is, however, a very important influence of the barrier width on a meV scale: it strongly influences the width of the minibands. Going from a barrier width of ~ 4 Å (defined by $m=2$ A atoms) to a width of ~ 34 Å ($m=32$) the ground state is shifted downwards by about 1 meV and its bandwidth decreases from 3 to 0.16 meV, i.e., almost by a factor of 20. For bandwidths in this range, miniband conduction breaks down completely,⁴³ since the slightest perturbation will localize the associated wave function: if Δ defines the range of random changes in the potential (α parameter of a lattice site) and W the bandwidth, then the parameter for Anderson localization⁴⁴ Δ/W will always be larger than the critical value if W is small enough. Due to localization of the wave function, electron transport will be dominated by tunneling through the barriers,⁴⁵ which is observed for three-dimensional superlattices with a ground-state bandwidth of ~ 0.4 meV.⁴⁶ The expected exponential decreases of the resonant tunneling current for increasing barrier width have been verified experimentally.⁴⁷

C. Effect of an electric field

The effect of an electric field on the electronic and excitonic structure of quasi-one-dimensional superlattices is investigated for a $(A_{16} B_{32})_x$ quantum-well structure (barrier width ~ 16 Å, well width ~ 96 Å). The bandwidths of the first minibands in the well are 0.7, 2.6, 4.8, 7.0, and 9.3 meV (by symmetry the same for valence and conduction bands). The separations between the bands are 115.6, 171.5, 207.2, and 225.9 meV, respectively. The lowest conduction band for the first confined electron lies at 1.1612 eV, 41.2 meV above the bottom of the well. The highest valence band defines the lowest band with respect to the bottom of the well for the first confined hole and lies at -1.2212 eV, against 41.2 meV above the bottom of the well.

Figure 4 shows the z dependence of the wave functions for the three lowest subbands in the well ($n=1, 2, 3$) by plotting the LCAO coefficients $c_{in}(k)$ [see Eq. (11)] and their squares for $k=0$ as a function of the site index i . They have amplitudes almost exclusively in the well region, but the amplitudes in the barrier are increasing from $n=1$ to $n=3$, indicating that the barrier becomes more transparent. Figure 4 also shows that the Bloch functions and, by virtue of Eq. (12), the Wannier functions for a single well have the same symmetry as the particle-in-a-box functions: with respect to the

center of the well the wave functions alternate between even (ground state $n=1, n=3,5$) and odd ($n=2,4$). This is corroborated in the numerical computation of the matrix elements $\langle W_n | z | W_m \rangle$ [see Eqs. (15) and (16)] where nonzero elements are obtained only if $(n-m)$ is odd.

In the presence of an electric field the second-order Stark shift of the first confined electron energy (lowest conduction miniband) and the first confined hole energy (highest valence miniband) is calculated using Eq. (13) and taking the next five states $m=2-6$ into account in the summation. The results for fields up to 20×10^4 V/cm are shown in Fig. 5. For the largest field the $m=4$ state still contributes ~ 0.1 meV, for all other fields the Stark shift is determined by the first term in the sum. For $E=20 \times 10^4$ V/cm the shift is ~ 13 meV, about the same order of magnitude as the shift for the first confined electron energy in a three-dimensional (3D) (GaAs-AlGaAs) quantum-well structure.²⁵ This shift is approximately ten times smaller than the separation between the first two minibands, so the application of perturbation theory is warranted.

The effect of an electric field on the electron and hole wave function is shown in Fig. 6. In the presence of the field the even ground state is admixed with higher-lying odd states [see Eq. (14)] which have amplitudes near the well walls. The electrons and hole wave functions are pulled apart, which weakens the electron-hole interaction and therefore the exciton binding energy. But due to the confinement there is still an appreciable overlap and binding. The binding energy has been computed using Eq. (19). The first trial value for $\gamma=5.6$ eV (ionization potential—electron affinity of Li) yielded too large a binding energy. $\gamma=2.8$ eV positions, for zero field, the

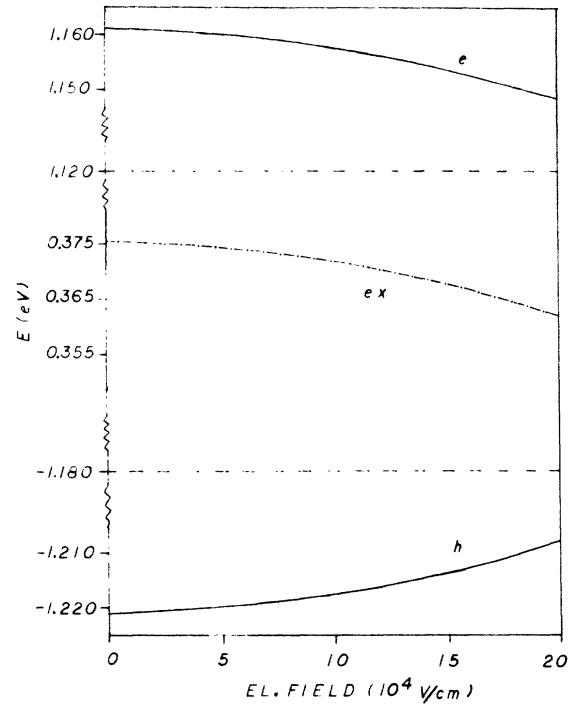


FIG. 5. Stark shift of the first confined electron (e) energy E_e in the lowest conduction miniband and first confined hole (h) energy E_h in the highest valence miniband and of the first exciton (ex) absorption peak (---). The bottom of the quantum wells for the electron and the hole in the $(A_{16}B_{32})_x$ superlattice are indicated by dashed lines.

first exciton peak at 0.37 eV with a binding energy of 785.4 meV, which is about halfway in the gap as predicted by the *ab initio* calculations for superlattices with smaller unit cells, and is a sufficient approximation for all practical purposes of this first qualitative study. As

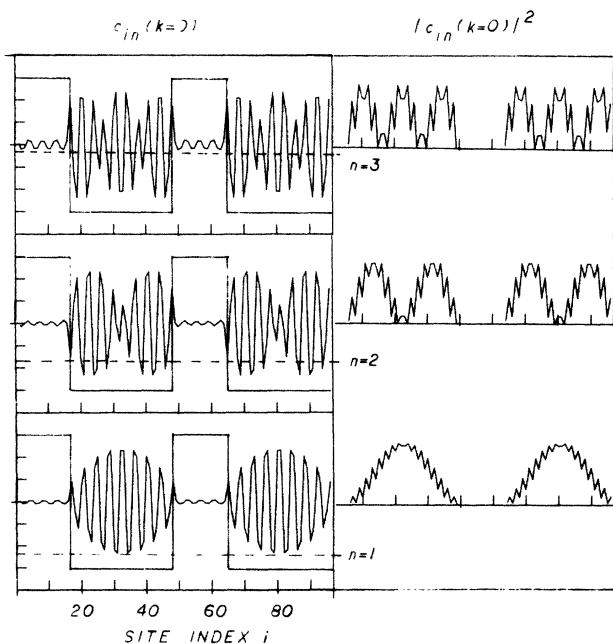


FIG. 4. The wave functions for the three lowest subbands ($n=1,2,3$) in the well of a $(A_{16}B_{32})_x$ superlattice. The LCAO coefficients $c_{in}(k)$ [see Eq. (11)] and their squares are plotted as a function of the site index i for $k=0$.

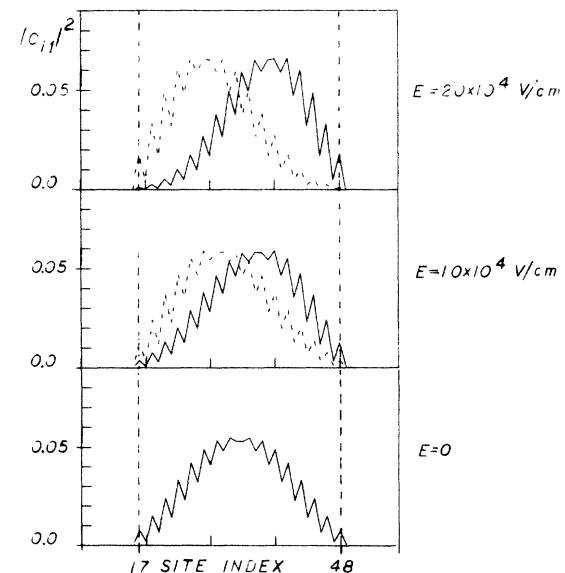


FIG. 6. Wave-function amplitudes [squares of the LCAO coefficients of the Wannier function as defined by Eq. (12)] vs site index for the first confined electron (solid line) and hole (dashed line) in a $(A_{16}B_{32})_x$ superlattice for various electric field strengths.

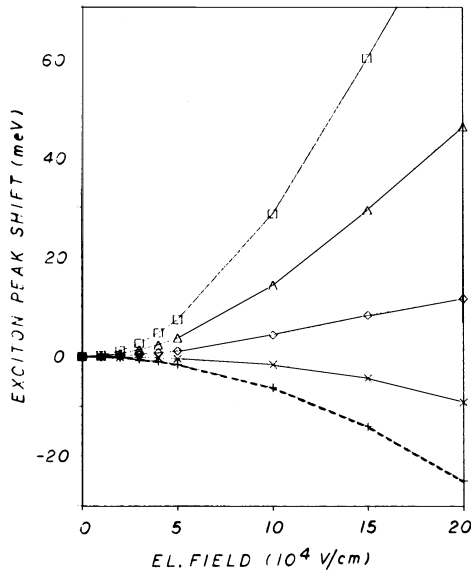


FIG. 7. Shift of the exciton peak position with applied field for various zero-field exciton binding energies E_{EXB}^0 if Eq. (19) is used together with the perturbed wave functions from Eq. (14). \square , $E_{\text{EXB}}^0 = 785$ meV ($\gamma = 2.8$ eV); \triangle , $E_{\text{EXB}}^0 = 563$ meV ($\gamma = 1.4$ eV); \diamond , $E_{\text{EXB}}^0 = 380$ meV ($\gamma = 0.7$ eV); \times , $E_{\text{EXB}}^0 = 239$ meV ($\gamma = 0.35$ eV); and $+$, $E_{\text{EXB}}^0 = 46$ meV ($\gamma = 0.05$ eV). The dashed line is the red shift as calculated from Eq. (28).

already mentioned in Sec. II C the first way of applying perturbation theory to calculate the Stark shift of the exciton peak fails. As illustrated in Fig. 7, it leads to a blue shift for large zero-field exciton binding energies. For an electron-hole system that is symmetric at zero field, this is unphysical, as is pointed out in footnote 53 of Ref. 25. Using the second approach [Eqs. (26)–(28)] a red shift of ~ 25 meV for 20×10^4 V/cm is obtained (see Fig. 5 and dashed curve in Fig. 7), comparable to the shifts calculated and observed in 3D quantum-well structures.²⁵

IV. SUMMARY AND CONCLUSIONS

In this paper we have studied for the first time the electronic structure of copolymers with a periodic se-

quence $(A_m B_n)_x$ of m constituent monomers A and n monomers B which represent prototypes of quasi-one-dimensional superlattices. An LCAO methodology based on Wannier functions has been developed for the calculation of the effect of an electric field on the electronic and excitonic structure of these quantum-well structures. Instead of using the empirical form of the equations, *ab initio* results can be obtained by substituting first-principle Wannier functions (calculating dipole moment expectation values for the computation of the Stark shift and two-electron integrals for the exciton binding energy). Tight-binding (Hückel) calculations have been presented together with Hartree-Fock results to assess the importance of self-consistent field effects. The splitting into subbands, the bandwidths, and the number of subbands in the well have been investigated as a function both of the well and the barrier width. The number of minibands, their bandwidths, and their position with respect to the bottom of the well are determined by the well width. An additional decrease in the bandwidths is obtained by increasing the barrier width.

The Stark shift of the first confined one-particle electron and hole energies, the perturbed Wannier functions, and the shift of the first exciton absorption peak have been calculated using perturbation theory. The results show that—up to second-order perturbation theory—the only contribution to the shift is the shift of the one-particle electron and hole minibands. A red shift similar to the one observed in three-dimensional quantum-well structures is obtained. Since the exciton binding energies in polymeric materials are much larger (~ 800 meV or by a factor of 100) than in typical 3D superlattices they are less perturbed by the applied electric field (10^5 V/cm corresponds to 100 meV potential difference across 100 Å). The results indicate that polymeric superlattices would be excellent materials for optical applications in which high electric fields play a role.

ACKNOWLEDGMENTS

Stimulating discussions with Professor P. Otto and Professor M. Huberman and the financial support of the Deutsche Forschungsgemeinschaft (Project No. Se 463/1-1) are gratefully acknowledged.

¹For a review, see, for example, L. L. Chang and L. Esaki, in *Progress in Crystal Growth and Characterization*, edited by B. R. Pamplin (Pergamon, Oxford, 1979), Vol. 2, p. 3; R. Dingle, in *Festkörperprobleme*, edited by J. Treusch (Pergamon, New York, 1975), Vol. 15, p. 21; L. Esaki, in *Proceedings of the 17th International Conference on the Physics of Semiconductors*, edited by J. D. Chadi and W. A. Harrison (Springer-Verlag, New York, 1984), p. 473.
²N. Holonyak, Jr., R. M. Kolbas, R. D. Dupuis, and P. D. Dapkus, *IEEE J. Quantum Electron.* **16**, 170 (1980).
³D. A. B. Miller, D. S. Chemla, T. C. Damen, A. C. Gossard, W. Wiegmann, T. H. Wood, and C. A. Burrus, *Appl. Phys. Lett.* **45**, 13 (1984).
⁴D. S. Chemla, D. A. B. Miller, P. W. Smith, A. C. Gossard, and W. Wiegmann, *IEEE J. Quantum Electron.* **20**, 265 (1984).

⁵See, for example, F. L. Carter, NRL Mem. Report No. 4335, 1980 (unpublished); *Physica* **10D**, 175 (1984).
⁶K. Kanazawa, A. F. Diaz, M. T. Krounbi, and G. B. Street, *Synth. Metals* **4**, 119 (1983).
⁷O. Inganäs, B. O. Liedberg, and W. U. Chang-ru, *Synth. Metals* **11**, 239 (1985).
⁸A. K. Bakhshi, J. Ladik, and M. Seel, *Phys. Rev. B* **35**, 704 (1987).
⁹R. Dingle, W. Wiegman, and C. H. Henry, *Phys. Rev. Lett.* **33**, 827 (1974).
¹⁰R. Tsu, L. L. Chang, G. A. Sai-Halasz, and L. Esaki, *Phys. Rev. Lett.* **34**, 1509 (1975).
¹¹H. Bluyssen, J. C. Maan, P. Wyder, L. L. Chang, and L. Esaki, *Solid State Commun.* **31**, 35 (1979).
¹²G. Bastard, *Phys. Rev. B* **24**, 5693 (1981); **25**, 7584 (1982).
¹³W. T. Masseling, P. J. Pearah, J. Klem, C. K. Peng, H. Mor-

- koc, G. D. Sanders, and Y.-C. Chang, *Phys. Rev. B* **32**, 8027 (1985).
- ¹⁴G. A. Sai-Halasz, L. Esaki, and W. A. Harrison, *Phys. Rev. B* **18**, 2812 (1978).
- ¹⁵J. N. Schulman and Y.-C. Chang, *Phys. Rev. B* **31**, 2056 (1985); Y.-C. Chang and J. N. Schulman, *ibid.* **31**, 2069 (1985).
- ¹⁶J. A. Moriarty and S. Krishnamurthy, *J. Appl. Phys.* **54**, 1892 (1983).
- ¹⁷I. Ivanov and J. Pollmann, *Solid State Commun.* **32**, 869 (1979).
- ¹⁸D. Ninno, M. A. Gell, and M. Jaros, *J. Phys. C* **19**, 3845 (1986).
- ¹⁹A. Elci, *Phys. Rev. B* **34**, 8616 (1986).
- ²⁰D. L. Smith and C. Mailhiot, *Phys. Rev. B* **33**, 8345 (1986).
- ²¹C. Mailhiot and D. L. Smith, *Phys. Rev. B* **33**, 8360 (1986).
- ²²C. Mailhiot and D. L. Smith, *Phys. Rev. B* **35**, 1242 (1987).
- ²³E. J. Austin and M. Jaros, *Phys. Rev. B* **31**, 5569 (1985).
- ²⁴G. Bastard, E. E. Mendez, L. L. Chang, and L. Esaki, *Phys. Rev. B* **28**, 3241 (1983).
- ²⁵D. A. B. Miller, D. S. Chemla, T. C. Damen, A. C. Gossard, W. Wiegmann, T. H. Wood, and C. A. Burrus, *Phys. Rev. Lett.* **53**, 2173 (1984); *Phys. Rev. B* **32**, 1043 (1985).
- ²⁶M. Matsuura and T. Kamizato, *Phys. Rev. B* **33**, 8385 (1986).
- ²⁷G. Del Re, J. Ladik, and G. Biczó, *Phys. Rev.* **155**, 997 (1967); J. M. André, L. Gouverneur, and G. Leroy, *Int. J. Quantum Chem.* **1**, 427 (1967).
- ²⁸S. Suhai, *Phys. Rev. B* **29**, 4570 (1984).
- ²⁹Y. Takeuti, *Prog. Theor. Phys.* **18**, 421 (1957).
- ³⁰E. A. Pschenichnov, *Fiz. Tverd. Tela (Leningrad)* **4**, 1113 (1962) [*Sov. Phys.—Solid State* **4**, 819 (1962)].
- ³¹C. B. Duke, *Tunneling in Solids* (Academic, New York, 1969), p. 79.
- ³²See also J. Callaway, *Quantum Theory of the Solid State* (Academic, New York, 1974), p. 545.
- ³³See, for example, A. Karpfen, *Theor. Chim. Acta* **50**, 49 (1978), and references therein.
- ³⁴W. J. Hehre, R. F. Stewart, and J. A. Pople, *J. Chem. Phys.* **51**, 2657 (1969).
- ³⁵C. A. Coulson, *Proc. R. Soc. London, Ser. A* **164**, 383 (1938); L. Salem, *The Molecular Orbital Theory of Conjugated Systems* (Benjamin, New York, 1966); G. F. Kventzel and Y. A. Kruglyak, *Theor. Chim. Acta* **12**, 1 (1968); W. P. Su, J. R. Schrieffer, and A. J. Heeger, *Phys. Rev. B* **22**, 2099 (1980).
- ³⁶See, for example, J. Ladik, *Quantemchemie* (Enke, Stuttgart, 1973).
- ³⁷See, for example, R. G. Parr, *The Quantum Theory of Molecular Structure* (Benjamin, New York, 1963).
- ³⁸K. Nishimoto and N. Mataga, *Z. Phys. Chem. (Frankfurt am Main)* **12**, 335 (1957).
- ³⁹W. E. Pickett, S. G. Louis, and M. L. Cohen, *Phys. Rev. Lett.* **39**, 109 (1977).
- ⁴⁰G. A. Baraff, J. A. Appelbaum, and D. R. Hamann, *J. Vac. Sci. Technol.* **14**, 999 (1977).
- ⁴¹W. A. Harrison, *J. Vac. Sci. Technol.* **14**, 1016 (1977).
- ⁴²M. Tsuchiya and H. Sakaki, *Appl. Phys. Lett.* **49**, 88 (1986).
- ⁴³R. F. Kazarinov and R. A. Suris, *Fiz. Tekh. Poluprovodn.* **6**, 148 (1972) [*Sov. Phys.—Semicond.* **6**, 120 (1972)].
- ⁴⁴P. W. Anderson, *Phys. Rev.* **109**, 1492 (1958).
- ⁴⁵F. Capasso, K. Mohammed, and A. Y. Chu, *Appl. Phys. Lett.* **48**, 478 (1986).
- ⁴⁶K. K. Choi, B. F. Levine, R. J. Malik, J. Walker, and C. G. Bethea, *Phys. Rev. B* **35**, 4172 (1987).
- ⁴⁷M. Tsuchiya and H. Sasaki, *Jpn. J. Appl. Phys.* **25**, L185 (1986).